УДК 551.463.8

© *М. И. Вдовин*[1]*, *И. А. Исаченко*[2], *А. А. Кандауров*[1], *Д. А. Сергеев*[1], *И. П. Чубаренко*[2]

© Перевод: *Е. С. Кочеткова*, 2021

[1]Институт прикладной физики РАН, 603950, ул. Ульянова, д. 46, г. Нижний Новгород, Россия
[2]Институт океанологии им. П.П. Ширшова РАН, 117997, Нахимовский пр., д. 36, г. Москва, Россия
*E-mail: arfirius@yandex.ru

ИССЛЕДОВАНИЕ ХАРАКТЕРИСТИК ТУРБУЛЕНТНОГО ПОГРАНИЧНОГО СЛОЯ PIV-МЕТОДОМ В УСЛОВИЯХ ЛАБОРАТОРНОГО МОДЕЛИРОВАНИЯ ТЕЧЕНИЯ НАД МОРСКИМ ДНОМ

Статья поступила в редакцию 06.03.2020, после доработки 24.07.2020

Настоящая работа посвящена разработке и применению системы измерения полей скорости течения методом Particle Image Velocimetry (PIV) (Анемометрии по Изображениям Частиц) в исследованиях турбулентного пограничного слоя в модернизированном гидродинамическом лотке Атлантического отделения Института океанологии им. П.П. Ширшова Российской академии наук. Работы проводились в рамках подготовки лабораторной установки к экспериментам по взмучиванию частиц микропластика со дна, покрытого естественным донным осадком. Эксперименты выполнялись при трех типах покрытия дна: крупный песок (1–1.5 мм), зёрна янтаря (3–4 мм), галька (1–2 см). Разработанная система PIV-измерений базируется на использовании цифровой камеры средней производительности и непрерывной лазерной подсветки. Эксперименты выполнялись в широком диапазоне скоростей потока (до 2 м/с), задаваемых частотой вращения насоса и положением регулирующей заслонки. Выполнены измерения профилей средней скорости, по наклону логарифмической части которых вычислялась динамическая скорость, которая, вместе с масштабом шероховатости дна, является одной из основных характеристик при исследовании процессов седиментации/взмучивания. Динамические скорости для песка и янтаря оказались близкими друг к другу, и значительно меньше, чем для гальки. Масштаб шероховатости для гальки, как и ожидалось, оказался максимальным. Янтарь в экспериментах не только моделировал дно промежуточной шероховатости, но также, из-за своей относительно малой плотности (1.07 г/см^3), позволил наблюдать начало движения частиц при небольших скоростях потока — меньших, чем необходимо для начала движения песка. Сравнение результатов наблюдений с известными данными А. Шильдса о пороге взмучивания янтаря показывают их хорошее согласие. Одним из основных преимуществ PIV-измерений в последующих экспериментах по исследованию динамики МП, можно считать возможность практически мгновенного измерения характеристик течения в пограничном слое с одновременным отслеживанием динамики добавленных на поверхность дна частиц МП.

Ключевые слова: турбулентный пограничный слой, лабораторное моделирование, взмучивание, PIV, микропластик.

© *M. I. Vdovin*[1]*, *I. A. Isachenko*[2], *A. A. Kandaurov*[1], *D. A. Sergeev*[1], *I. P. Chubarenko*[2]

© Translation: *E. S. Kochetkova*, 2021

[1]Institute of Applied Physics of RAS, 603950, Ulyanov Str., 46, Nizhny Novgorod, Russia
[2]Shirshov Institute of Oceanology of RAS, 117997, Nahimovsky Pr., 36, Moscow, Russia
*E-mail: arfirius@yandex.ru

STUDY OF THE CHARACTERISTICS OF THE TURBULENT BOUNDARY LAYER BY THE PIV-METHOD UNDER LABORATORY MODELLING OF THE FLOW ABOVE THE SEABED

Received 06.03.2020, in final form 24.07.2020

This article is devoted to the development and application system for Particle Image Velocimetry (PIV) measurements of velocity fields in a turbulent boundary layer within experiments carrying out on the modified hydrodynamic flume of the Atlantic Branch of the Shirshov Institute of Oceanology of the Russian Academy of Sciences. This study is concerned with the preparation

Ссылка для цитирования: *Вдовин М.И.*, *Исаченко И.А.*, *Кандауров А.А.*, *Сергеев Д.А.*, *Чубаренко И.П.* Исследование характеристик турбулентного пограничного слоя PIV-методом в условиях лабораторного моделирования течения над морским дном // Фундаментальная и прикладная гидрофизика. 2021. Т. 14, № 2. С. 29–38. doi: 10.7868/S2073667321020039

For citation: *Vdovin M.I.*, *Isachenko I.A.*, *Kandaurov A.A.*, *Sergeev D.A.*, *Chubarenko I.P.* Study of the Characteristics of the Turbulent Boundary Layer by the PIV-Method under Laboratory Modelling of the Flow above the Seabed. *Fundamentalnaya i Prikladnaya Gidrofizika*. 2021, 14, 2, 29–38. doi: 10.7868/S2073667321020039

of laboratory setup for investigations on the initiation of motion of microplastic particles from the bottom covered with natural bottom sediment. The conditions of three types of bottom material (coarse sand (1–1.5 mm), amber grains (3–4 mm), pebbles (1–2 cm)) were investigated. The developed system of PIV-measurements uses a digital camera of medium framerate and continuous wave laser illumination. The experiments were performed in a wide range of flow velocities, up to 2 m/s, controlled by a pump rate and a control valve position. Average velocity profiles were measured, and the slope of their logarithmic part was used to calculate the corresponding friction velocity. The friction velocity and the bottom roughness are the crucial parameters for the assessment of sedimentation/initiation of motion processes. Friction velocities over sand and amber appear to be similar and significantly smaller than that for pebbles. The pebble roughness scale turned out to be the maximum, as expected. The amber simulated the bottom of intermediate roughness. For this case, due to its relatively low density (1.07 g/cm^3), we observed the beginning of particle motion at velocities lower than those necessary for the initiation of sand grain movement. There was a good agreement between the observed threshold of motion for amber with available data obtained by A. Shields. The advantage of PIV-measurements for further investigations of the microplastic dynamics is the possibility of simultaneous measurement of almost instant velocity parameters in the boundary layer together with the observation of microplastic particles added at the bottom surface.

Key words: microplastics, laboratory experiment, boundary layer, initiation of motion, PIV.

1. Introduction

Investigation of the fluid flow properties in the turbulent boundary layer flow (further we use the simplified term "boundary layer") over a solid bottom with various characteristics is a crucial and complex fundamental hydrodynamic problem with numerous various practical applications. The history of flow dynamics studies in laboratory conditions commenced a hundred years ago with experiments of Ludwig Prandtl [1]. Strong flow velocity gradients close to the hard surface and intense fluctuations in a turbulent boundary layer stimulated the development of measurement techniques in hydrodynamic experiments with high spatial and temporal resolution. At various times, both contact methods, including hot-wire anemometry [2] and remote methods: acoustic/laser-Doppler methods [3, 4], as well as a technique based on visualization of flows, were used to study the turbulent boundary layer, including the most modern of them — PIV-method (Particle Image Velocimetry) [5–7]. There are various ways to model the underlying surface in laboratory experiments. When investigating open channels to simulate industrial and natural systems, including conditions in the hydrosphere objects (rivers, seas, oceans), from the installation of model obstacles (cubes, hemispheres, cylinders, etc.) on a smooth tray bottom, arranged chaotically or orderly (in a row or staggered order) [5, 6], up to complete coverage by artificial or natural material usual for real conditions (silt, sand, pebbles, etc.) [4, 7].

The problem of studying the initiation of motion/sedimentation of solid particles in the boundary layer deserves a special note. Investigations of bottom erosion's physical mechanisms began with fundamental works in the 1930s (see [8, 9]). The main goal of those studies was to obtain a criterion for initiation of motion/sediment movement initiation prediction. The complexity of the problem later led to the appearance of numerous theoretical and experimental works (see [10]), including studies of the criteria for the onset of movement of both homogeneous and mixed sediments (see, for example, [11, 12]). The review of historical and modern research in this area, given in [13], allows us to conclude that, despite significant efforts made, the final solution to the problem is far from complete. Recently, similar questions have arisen in connection with the need for a qualitative and quantitative description of a newly emerged environmental problem of microplastic (MP) dynamics in the hydrosphere of our planet (see [14]). Usually, MP particles are fragments of synthetic polymers less than 5 mm in size, of various shapes: three-dimensional chunks, flat flakes, fine flexible threads, etc. The density of MP particles material varies in the range of 0.01–2.3 g/cm^3; however, the densities of most common types of polymers are comparable to seawater (see [15]). Ballent with co-authors [16] performed the first experimental studies on the dynamics of MP particles on the seabed bottom. That paper presents the results of laboratory measurements of the flow parameters for the initiation of motion and re-deposition of "natural" (collected on the seashore) plastic pellets with a characteristic size of 3.3–5.1 mm and a density of 1.06–1.13 g/cm^3. Other researchers [17] estimated critical level shear stresses values for the displacement of 14 types of MP particles with different shapes and densities for five types of bottom type. Their empirical formula for the critical Shields parameter was based on an analogy with bimodal sediment [18]. Still, some of the results remained unexplained by the authors within the framework of the considered theories. Admittedly, these two studies constitute an exhaustive review of experimental studies of MP transport at the seabed. Thus, the relevance of further research is evident.

The necessity to design a laboratory setup for experiments on the initiation of motion of MP was the main motivation for this study. Laboratory modelling is well suited for MP initiation of motion process investigations for the bottom forming elements (granules) and the particles specially placed on the bottom surface. Modelling provides control and reproducibility of experimental conditions (flow characteristics, bottom parameters, and microparticles)

and allows a simultaneous detailed study of the MP dynamics and flow parameters. In these experiments, the principal characteristic of a flow is turbulent shear stress (see [19]) or turbulent momentum flux, which is expressed in terms of the so-called friction velocity:

$$\tau = \rho\langle u'w'\rangle = \rho u_*^2, \quad (1)$$

where ρ is water density, u' and w' are horizontal and vertical components of velocity fluctuations, correspondingly, u_* is friction velocity (shear stress).

Thus, based on definition (1), to calculate the shear stress, the measurements of the fluctuation components of the horizontal and vertical velocities are needed. However, the friction velocity (and thus, shear stress) is calculated using the mean velocity flow profile data. Indeed (see, for example, [20]), in the developed turbulent boundary layer, the velocity profile between the viscous sublayer and the middle part of the profile has a logarithmic part (constant turbulent shear stress):

$$U(z) = \frac{u_*}{\kappa}\ln\left(\frac{z}{z_0}\right), \quad (2)$$

where κ is a Karman's numerical constant, which is usually considered equal to 0.4, and z_0 is the roughness height for the bottom surface. Thus, friction velocity can be calculated by determining the velocity profile slope in the logarithmic part of the boundary layer. In this work, we will use this approach and PIV-method to measure the flow velocity.

The PIV-method is preferable to point (contact and distance) methods because it significantly reduces the time for obtaining information due to the large area of measurement of the current velocity. It also allows measurements very close to the bottom surface, which is especially important for rough surfaces. Therefore, the PIV-method was chosen for studies on the modified hydrodynamic flume of the Atlantic Branch of the Shirshov Institute of Oceanology of the Russian Academy of Sciences (AO IO RAS), which was proposed for detailed measurements of the flow characteristics in a wide range of operating modes for various simulated seabed types.

The main aim of the research was to estimate the turbulent shear stress and the roughness height parameter in various regimes in the flume. We also studied the threshold characteristics of flows at which the initiation of motion of the simulated seabed granules began to move in the flume, including those which physical parameters similar to the MP.

The article is structured as follows. The first section describes the experimental setup itself, the PIV-system, and the measurement technique. The second section presents a technique for processing images and acquired data. The final section analyzes the results.

2. Description of the experimental setup, PIV system and measurement procedure

The main characteristics of the plexiglass hydrodynamic flume are as follows: total length of 10 m, cross-section 33 × 33 cm. The experiments were carried out on a flat bottom with three types of coverage: very coarse sand (1–1.5 mm), amber grains (3–4 mm), and pebbles (1–2 cm) according to the scale proposed in [21]. Fig. 1 shows photographs of a hydrodynamic flume with all three types of seabed models. Only part (1.5 m) of the bottom contained amber, while the rest of the flume carried natural granules of the same size (3–4 mm). These sediment types simulate various bottom roughness, and hence, different flow patterns, for comprehensive testing of the PIV-system capability. Besides, the use of amber as a bottom coating material, the density of which is much lower than the density of typical natural sediments, makes it possible to compare observations of the beginning of its movement with known measurements [8] even at low flow rates, which is a good test of the system's suitability for further experiments with MP particles.

The water level (the distance from the upper boundary of seabed model to the water surface) was set as a mean value between measurements in first and last sections of the flume because of a slight slope of the free surface due to the drain design. It varied depending on the flow regime and bottom characteristics from 12.5 to 18.8 cm. There were two options to control the velocity profile characteristics in the flume: 1) the primary method was an adjustment of the rotation frequency of the circulation pump, 2) an additional method used to obtain the maximum flow rates was to vary the height of the supporting shutter at the end of the flume, which regulates the drain of water into the intermediate volume.

A dedicated system was developed for velocity measurements with the PIV-method on a hydrodynamic flume (see fig. 3, *a*, *b*) with continuous wave (CW) laser illumination (similar to [22]). To visualize the flow, the water was seeded with calibrated polyamide microparticles with a characteristic size of 50 μm and a density of 1.02 g/cm^3 manufactured by Dantec, specially designed for PIV-measurements. A cylindrical lens formed the laser sheet (light

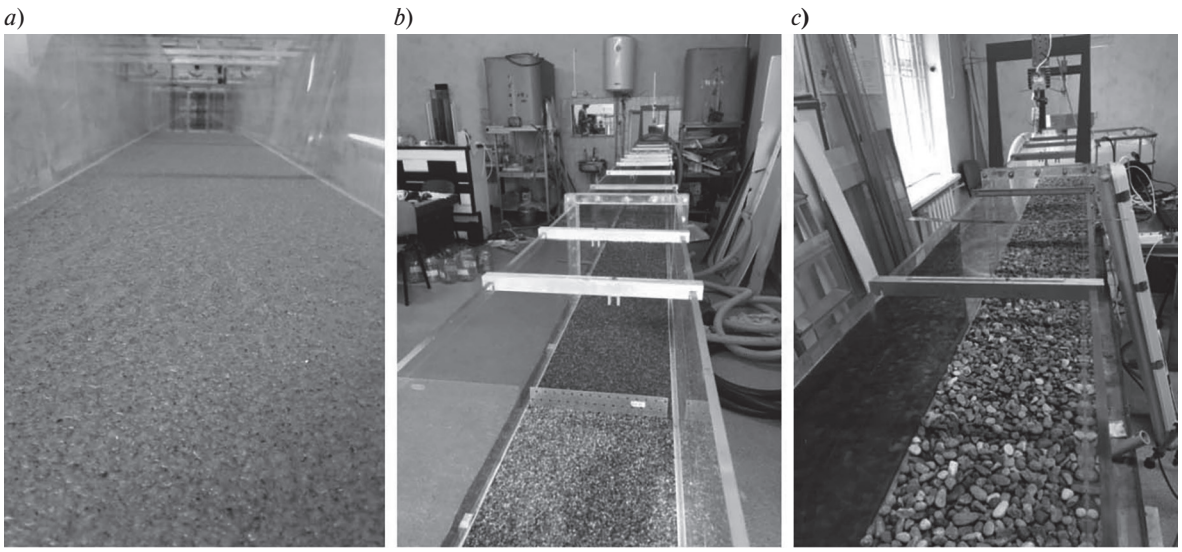

Fig. 1. Various types of seabed used in experiments at the hydrodynamic flume IO RAS: *a* — medium-grained sea sand, *b* —granules, a part of the bottom covered with amber of the same size, *c* — pebble bottom.

plane) with a focal length of 25 mm from a beam of a blue continuous-wave diode laser (LD450-G-2, beam diameter 3 mm, wavelength 450 nm, power 2 W). The laser was positioned vertically above the flume. A lens was installed between the laser and the flume on a special adjusting device. The distance from the cylindrical lens to the bottom of the flume was 59.5 cm. The width of the laser sheet above the area of the survey was about 2 cm, the thickness was about 3 mm. Baumer VCXU-23M camera was used for the filming of the visualized flow in the laser sheet. The framerate was 300–500 frames per second (with an increase in the velocity flow, the filming speed increased accordingly), the shutter speed was 1/2000 s, the recording length was 12000 frames, and the image scale varied 75.67 to 82.5 μm/pixel. Rearrangements of the camera during the entire period of the experiments caused a slight variation in the images' scale. The frame size remained constant — 128 × 1920 pixels. Thus, the vertical size of the shooting area varied from 145 to 160 mm. The observed area always covered the bottom to ensure velocity measurement in its immediate vicinity (see fig. 3, *c*). These illumination and video recording systems' parameters allowed measurements of velocities with the PIV-method in the range of up to 2 m/s using a medium framerate camera and a widely available miniature diode continuous laser (albeit in a relatively narrow region in the horizontal direction). The vertical size of the taken area often exceeded the water depth in the flume. In other cases, it lacked not more than 30 mm. Thus, it was possible to restore the vertical profiles of flow characteristics and find the shear stress (see Section 3 below).

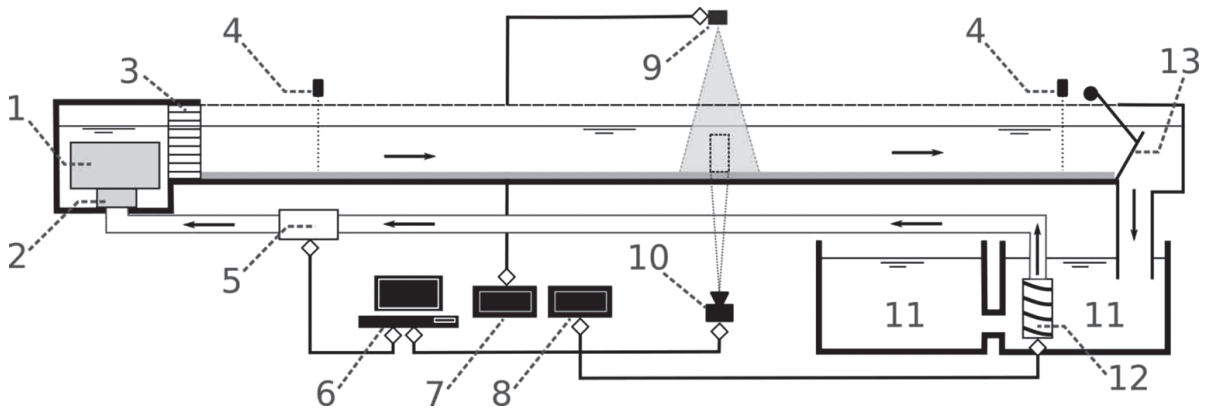

Fig. 2. Laboratory setup diagram. The numbers indicate: 1 — divider, 2— check valve, 3 — section for flow smoothing, 4 — water level control positions, 5 — flow rate gauge, 6 — computer for data processing, 7 — laser power supply, 8 — pump operation controller, 9 — laser with a light sheet optics, 10 — video camera, 11 — water circulation tanks, 12 — pump, 13 — shutter with height adjustment mechanism.

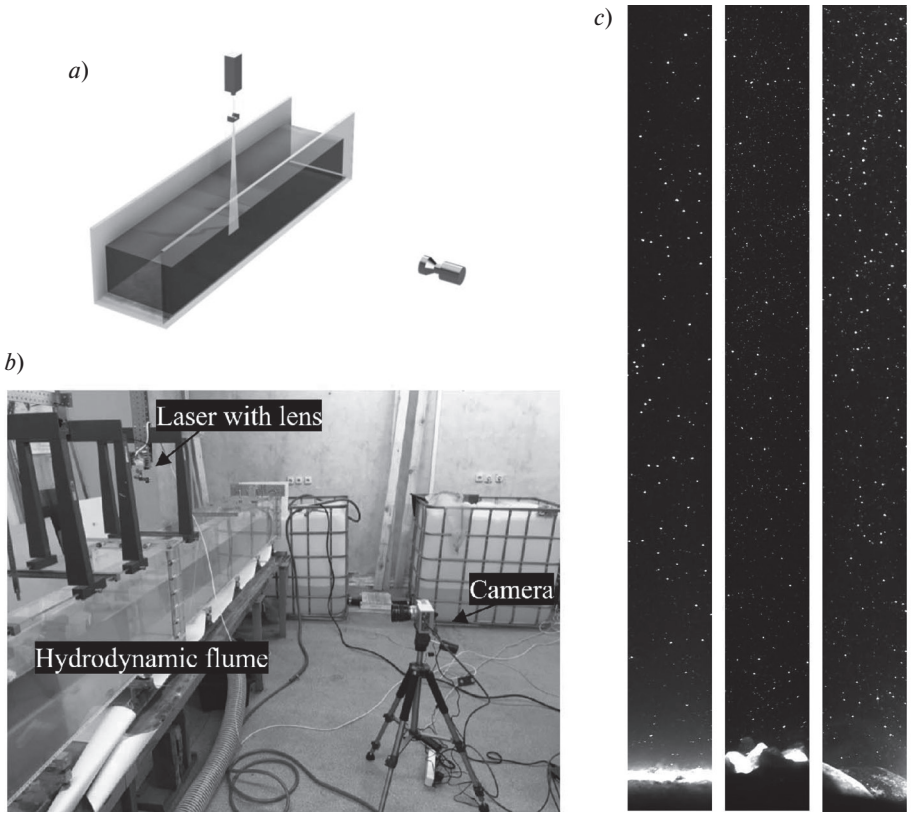

Fig. 3. Illustration of PIV-measurements: *a* — General 3D-scheme of the PIV-measurements, *b* —general view of the PIV-system installed on the hydrodynamic flume of the IO RAS, *c* —examples of the lower part of the frames of visualization in the laser sheet in PIV-measurements above different bottom: sand (*left*), amber (*centre*), pebbles (*right*).

We performed all measurements at one fixed distance from the beginning of the flume (628 cm). The upper edge of the shutter was 122 mm above the bottom in most experiments. The measurement scheme was as follows. Measurements started at low flow rates (minimum 11 Hz pump frequency), then frequency increased with an increment of 2, 3, or 4 Hz (depending on the experiment). In fig. 4, the actual values of the pump operating frequencies during velocity measurements are shown (see below). For experiments with sand, the maximum frequency was 39 Hz, with amber, it was 24 Hz, and with pebbles, it was 50 Hz. Thus, results of measurements correspond to the maximum in the profile of the mean flow velocity: 90 cm/s for sand, 58 cm/s for amber, 125 cm/s for pebbles with a raised shutter, and 200 cm/s for pebbles with a lowered shutter. For the case of a pebble, the risk of bottom erosion with a further increase in the velocity flow was insignificant; therefore, for better testing of the measurement system, experiments were also performed with an almost completely lowered shutter (height 10 mm at a maximum pump frequency of 50 Hz), which provided a significant increase, almost 1.5 times, of the flow velocity (see below fig. 4, *c*). The interval between each recording, and the interval before the recording after setting the mode (increasing the frequency), was at least 4 minutes. Three separate independent records for each regime made it possible to estimate the stability of the average flow parameters.

Observation of the seabed granules behaviour in the PIV-measurement zone was carried out visually with a detailed log of the surface particles' movement characteristics during the entire process of the pump frequency increase.

3. Technique for processing PIV images and data acquiring

The sequences of frames obtained by the PIV-method were processed using cross-correlation analysis (see [22]). Pairs of consecutive images were compared. An adaptive PIV-algorithm was used. At the first stage, preliminary velocity fields with low resolution were calculated on a grid with a cross-correlation function search for the interrogation window of 128 × 128 pixels with 50 % overlap. At the next stage, after filtering and interpolation, this data was used in the second stage to estimate the preliminary of displacement in cross-correlation processing with smaller interrogation windows to increase the resolution. At the final stage, the cross-correlation was calculated for windows

of 32 × 32 pixels with an overlap of 50 %, with the refinement of the cross-correlation function maximum using three points of the Gaussian approximation. The final spatial resolution was 16 pixels, or 1.3–1.4 mm, depending on the image scale (75.67–82.5 μm/pixel). This scale is less than the size of the smallest hot-wire sensing element of the Dantec Dynamics and almost four times smaller than the averaging volume of the Micro ADV Nortec ultrasonic velocity meter. Only LDA has similar resolution characteristics. Comparison with the median value for the entire time recording for each horizon in two passes was used for filtration of the PIV-results, with a three standard deviations threshold value of the bias components deviation from the median.

The obtained velocity fields were averaged over time and the horizontal coordinates. When averaging the velocity profile over time, we considered various intervals in the range from 0.03 to 40 seconds (the maximum recording time at a speed of 300 frames/s). Results show that an increase in the averaging periods, starting from 16 seconds, gives a difference between the obtained average profiles is less than 1 % for all measurements. The time taken to acquire the velocity profile is significantly less than scanning with point gauges.

The estimations of the accuracy of the PIV-method were based on the work [23]. We investigated the accuracy characteristics for a cross-correlation processing scheme similar to that used in our case. Research [23] presents the systematic error E_{rms} of displacement measurements concerning the following: 1) the mean diameter of the particle image d 2) the number of particles in the interrogation window N_I 3) the size of the final window D_{If} 4) the displacement gradient in the window, which was defined as the ratio $\Delta u/D_{If}$, where Δu is the difference in image displacements in pixels inside the window. Using these dependencies, we determined $E_{rms} = 0.16$ pixels, for the mean values that were in our studies: $d = 1.2$ pixels, $N_I = 13$, $\Delta u/D_{If} = 0.063$ at $D_{If} = 32$ pixels. For an image scale that varied in the range of 75.67–82.5 μm/pixel, the error will be, respectively, from 12.1 to 13.2 μm. When recalculating the displacement errors into velocity errors, it is important to account for the framerate variation from 300 to 500 frames/second (it grew with an increase in the current velocity). Accordingly, the velocity error varied in the range from 3.6 mm/s to 6.6 mm/s. These are estimates of the root-mean-square deviation of the measured value from the actual value at the point.

The generally accepted recommendation (see, for example, [24, 25]) for cross-correlation PIV-processing of sequential images without the integration windows shifting determines the maximum velocity measurement range of 200 cm/s. The image offset between two successive frames should not exceed a quarter of the initial integration window diagonal. In our case, for a window of 128 pixels, this threshold value was approximately 45 pixels. At a maximum speed of 200 cm/s, when the shooting speed was 500 frames per second, and the scale is 82.5 μm/pixel, the maximum displacement was 46 pixels, which practically coincides with the threshold value.

4. Analysis of the results

Figure 4 shows the mean velocity profiles obtained over the studied bottom types at various frequencies of the feed pump. For the bottom covered with pebbles (fig. 4, *c*), all velocity profiles are presented, including those that are very different (high speed), which correspond to the conditions mentioned above with a lowered shutter (height 10 mm) and a maximum pump frequency of 50 Hz. In a similar fig. 4, *d*, these last profiles are not shown for better perception and comparison with similar results for sand (fig. 4, *a*) and amber (fig. 4, *b*).

The friction velocity and the roughness scale were determined by approximating the lower (logarithmic) part of the profile by formula (2). The result of approximation is strongly affected by setting the position of the upper boundary of the logarithmic part. The higher the flow rate (velocity in the flume), the more strongly the velocity profile is deformed, lowering the boundary setting. Based on the best approximation in terms of the standard deviation, the boundary was set for each profile individually.

Figure 5, *a* shows the dependence of the obtained friction velocity u_* on the pump frequency. However, data on the modes with the maximum velocity for the pebble seabed with the shutter lowered, which was discussed above, are not given here. For this case, due to the strong deformation and small logarithmic section of the profile, the result of the approximation cannot be considered reliable. The dynamic velocity increases almost linearly (with a slight bend for a pebble seabed) with the increase in frequency. The magnitude of the friction velocity is slightly different for the conditions of sand and amber but is significantly lower for pebbles. In this case, the height of roughness for the bottom made of granules/amber is larger than for sand and is significantly smaller compared to pebbles (mean roughness values are marked in fig. 5, *b* by horizontal lines). The spread of values for the roughness scale significantly exceeds the spread of the results for the friction velocity. The reason for this, most likely, is that errors in determining the roughness parameter are exponentially related to errors in velocity measurements in individual profiles in accordance with formula (2).

Calculating the Shields parameter θ to compare observations of amber with the known data on its beginning of movement [8] was carried out according to the formula $\theta = \tau/((\rho_s - \rho_0)\, gd)$, where $\tau = \rho_0 u_*^2$ gs^2/cm, $\rho_s = 1.07$ g/cm^3 is

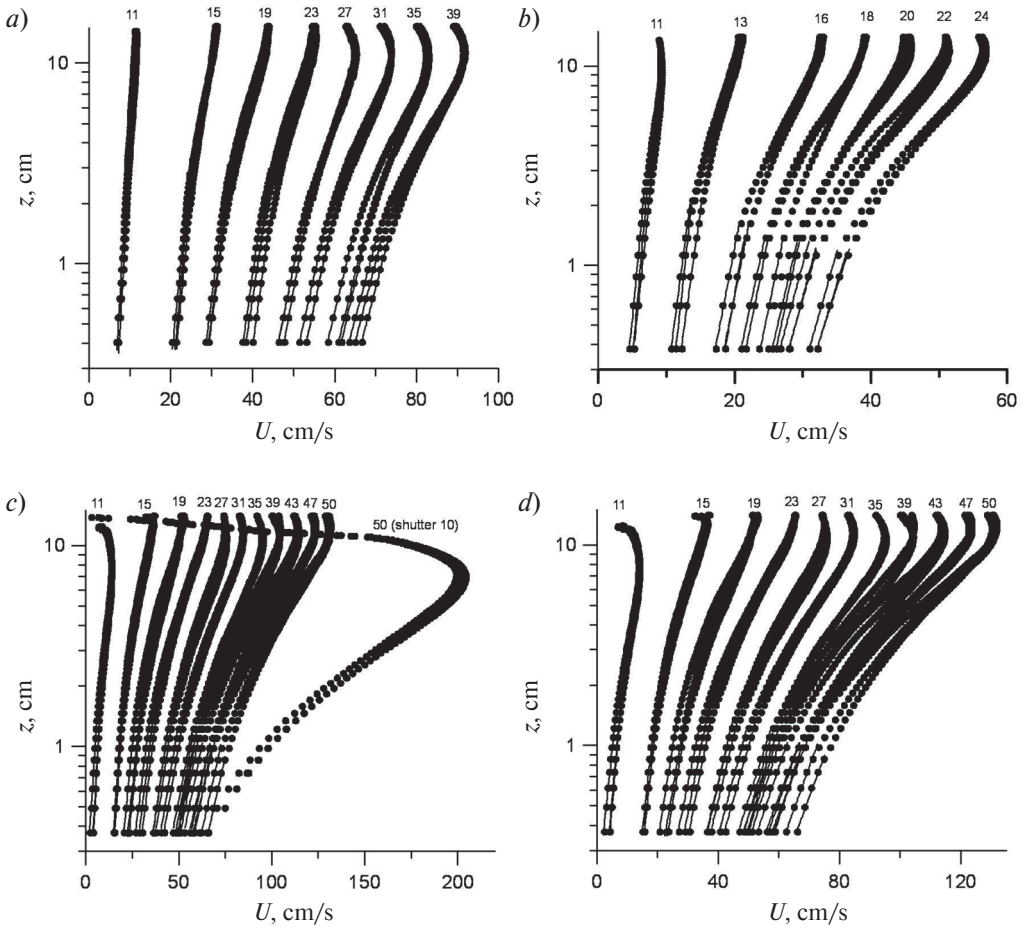

Fig. 4. Mean velocity profiles: *a* — for the sandy bottom, *b* — for the granule/amber bottom, *c* — for the pebble bottom, *d* — for the pebble bottom without maximum velocities with the shutter down. Dashed lines are the approximations in accordance with formula (2). The numbers in the graphs indicate the pump operating frequency.

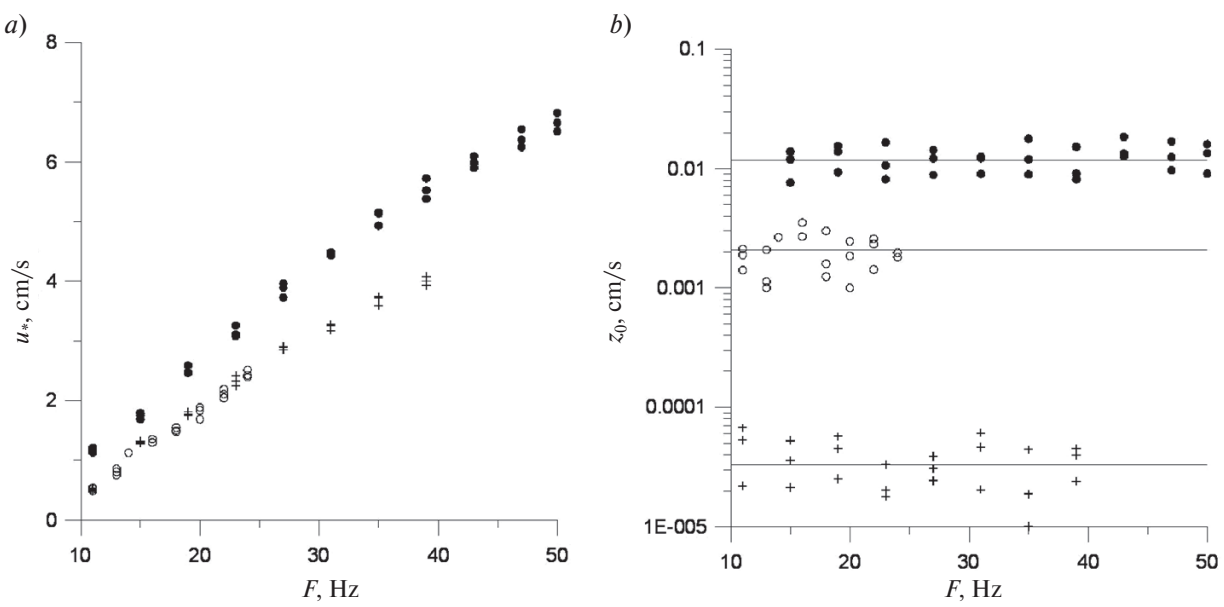

Fig. 5. Dependence on the frequency of the pump: *a* — the friction velocity, *b* — the roughness height. Symbols denote: + sand, ○ amber, • pebbles.

amber density, $\rho_0 = 1$ g/cm^3, $g = 980$ cm/s^2 is gravity acceleration module, $d = 3.5$ mm is particle size. Observations showed that at 11 Hz ($\theta = 0.011$), particle movements are still absent, but at 13 Hz ($\theta = 0.03$), single movements (displacement, swaying) are observed. This regime develops up to 16 Hz ($\theta = 0.05$) when the rolls of individual particles become steady, and vibration becomes ubiquitous. Subsequently, the bottom transport intensifies until the development of a steadily moving "river of particles" at 24 Hz ($\theta = 0.24$). For comparison: the beginning of the amber movement on the Shields diagram [8] is characterized by the values $\theta_{cr} = 0.03–0.04$. Though in our experiments, the beginning of particles' motion was determined qualitatively from visual observations, the comparability can be considered very good. Thus, the obtained measurements of the average flow are in a good agreement with the critical conditions of initiation of motion.

Even though the beginning of the movement of amber particles, which corresponding density to the ubiquitous polymer polystyrene and match MP particles in size (<5 mm), has been quite reliably determined, the experiments provide only a foundation for further studies of the process of MP transport in the marine environment. Indeed, the properties of MP particles (density, size, shape) differ significantly from the properties of bottom sediment material in natural conditions. Therefore, the critical motion value of the Shields parameter $\theta_{cr} = 0.03–0.04$, obtained for the displacement occurring of the amber grains (3–4 mm) at the bottom of the same particles, can characterize only the order of magnitude, for example, such a very similar situation: the beginning of the movement of polystyrene particles (close to amber density 1.05–1.07 g/cm^3, the same size 3–4 mm and similar shape) on the bottom, covered with natural particles of the same size and shape. On a sandy bottom, $\theta_{cr} < 0.03–0.04$ is characteristic for the movement beginning, while on coarse pebbles it may be unattainable in principle since small MP particles (relative to pebbles) are removed from the flow being buried deep in cracks between sediment particles. Due to their ability to register vortex formations above the coarse-grained sediment, the PIV-study methods are best suitable for investigation various mechanisms of initiation of motion of MP particles, especially considering the exceptional variety of shapes.

5. Conclusion and discussion

To study the process of initiation of motion of seabed particles and the dynamics of MP particles in laboratory simulation on the modified hydrodynamic flume of the AB IO RAS, a system for PIV-measurement has been developed based on the use of CW laser illumination and a digital camera of the medium frame rate. The new system demonstrated spatial resolution higher than a hot-wire and ultrasonic Doppler gauges within the investigations of the velocity fields in the turbulent boundary layer. It should be noted that the undoubted advantage of the PIV-method in comparison with contact measurements is the possibility of a faster measurement of the velocity profile. This is useful in further studies of the MP particles' dynamics when it is necessary to simultaneously control both the parameters of particle motion and the characteristics of flows near the bottom.

The developed system was used to measure the mean velocity profiles in the entire range of flow rates in the flume with three types of simulated bottom material: sand, granules/amber, and pebbles. The dependencies of the friction velocity and the bottom roughness parameter on the pump frequency are determined. The critical Shields parameter for amber 0.03 was estimated based on the measured flow characteristics and visual observations of the bottom state. It is in good agreement with the results presented in the literature. The parameters of amber particles are close to the characteristics of MP fragments seeding in the marine environment: the buoyancy close to the polystyrene, some grades of polypropylene, and polyphenylene oxide; the size is less than 5mm, and the shape is irregular. Thus, the applied PIV-measurement technique is suitable for further investigation of the dynamics of MP particles at the bottom.

6. Funding

The study was carried out under the support of the Russian Foundation for Basic Research (Grant No. 19–35–50028), which ensured the long-term work of the young scientist MV in the laboratory of Marine physics of the AB IO RAS. The development of a PIV measurement system, flow measurements, processing, and analysis of their results were supported by the RFBR grant no. 19–35–50028. Preparation of the hydrodynamic flume, the participation of II and ICh in experiments, discussion, and processing of results were supported by the Russian Science Foundation, grant No. 19–17–00041.

Литература

1. *Prandtl L.* Bemerkungen über den Wärmeübergang im Rohr // Physik. Zeitschr. 1928. V. 29, 487.
2. *Klewicki J.*, *Falco R.* On accurately measuring statistics associated with small-scale structure in turbulent boundary layers using hot-wire probes // J. Fluid Mech. 1990. V. 219. P. 119–142. doi: 10.1017/S0022112090002889

3. *Balachandar R.*, *Bhuiyan F.* Higher-order moments of velocity fluctuations in an open-channel flow with large bottom roughness // J. Hydraul. Eng. 2007. V. 133(1). P. 77–87. doi: 10.1061/(ASCE)0733–9429(2007)133:1(77)
4. *Faruque M.A.A., Balachandar R.* Roughness effects on turbulence characteristics in an open channel flow // Can. J. Civ. Eng. 2010. V. 37. P. 1600–1612. doi: 10.1139/L10–098
5. *Guala M.* et al. Vortex organization in a turbulent boundary layer overlying sparse roughness elements // J. Hydraul. Res. 2012. V. 50(5). P. 465–481. doi: 10.1080/00221686.2012.729229
6. *Qi M.* et al. Roughness effects on near-wall turbulence modelling for open-channel flows // J. Hydraul. Res. 2018. V. 56(5). P. 648–661. doi: 10.1080/00221686.2017.1399931
7. *Spiller S.M.* et al. Form-induced stress in non-uniform steady and unsteady open channel flow over a static rough bed // Int. J. of Sediment Res. 2015. V. 30(4). P. 297–305. doi: 10.1016/j.ijsrc.2014.10.002
8. *Shields A.* Application of similarity principles and turbulence research to bed-load movement // Hydrodynamics Laboratory. Publ. No. 167, U.S. Dept. of Agr., Soil Conservation Service Cooperative Laboratory, California Institute of Technology, Pasadena, California.
9. *Hjulstrøm F.* Transportation of debris by moving water // Recent Marine Sediments: A Symposium / Ed. Trask, P.D. Tulsa, Oklahoma: American Association of Petroleum Geologists, 1939. P. 5–31.
10. *van Rijn L.C.* Principles of sediment transport in rivers, estuaries and coastal seas. Amsterdam: Aqua Publications, 1993. 690 p.
11. *Shvidchenko A.B., Pender G.* Flume study of the effect of relative depth on the incipient motion of coarse uniform sediments // Water Resour. Res. 2000. V. 36, N2. P. 619–628.
12. *McCarron C.J., Van Landeghem K.J., Baas J.H., Amoudry L.O., Malarkey J.* The hiding-exposure effect revisited: a method to calculate the mobility of bimodal sediment mixtures // Marine Geology. 2019. V. 410. P. 22–31.
13. *Yang Y., Gao S., Wang Y.P., Jia J., Xiong J., Zhou L.* Revisiting the problem of sediment motion threshold // Cont. Shelf Res. 2019. 103960.
14. *Chubarenko I.* et al. Behavior of Microplastics in Coastal Zones // Microplastic Contamination in Aquatic Environments / Ed. by Eddy Y. Zeng. Elsevier, 2018. P. 175–223.
doi: 10.1016/B978–0–12–813747–5.00006–0
15. *Geyer R., Jambeck J.R., Law K.L.* Production, use, and fate of all plastics ever made // Sci. Adv. 2017. V. 3(7). e1700782.
16. *Ballent A.* et al. Modelled transport of benthic marine microplastic pollution in the Nazaré Canyon // Biogeosciences. 2013. V. 10(12). 7957.
17. *Waldschläger K., Schüttrumpf H.* Erosion Behavior of Different Microplastic Particles in Comparison to Natural Sediments // Env. Sci. Technol. 2019. V. 53(22). P. 13219–13227.
18. *Wilcock P.R.* Methods for estimating the critical shear stress of individual fractions in mixed-size sediment // Water Resour. Res. 1988. V. 24. P. 1127–1135.
19. *Sherman D.* et al. Sediments and Sediment Transport // Treatise on Geomorphology / Ed. by John F. Shroder. Academic Press, 2013. P. 233–256.
doi: 10.1016/B978–0–12–374739–6.00013–0
20. *Hinze J.O.* Turbulence: an introduction to its mechanism and theory. New York: McGraw-Hill, 1959. 586 p.
21. *Wentworth C.K.* A scale of grade and class terms for clastic sediments // J. Geology. 1922. 30(5). P. 377–392.
22. *Сергеев Д.А.* Измерительный комплекс для исследования течений жидкости методом пробных частиц на основе твердотельного лазера с диодной накачкой // Приборы и техника эксперимента. 2009. № 3. С. 138–144.
23. *Bolinder J.* On the accuracy of digital particle image velocimetry system // Lund Inst. of Tech., Tech. Div. of Fluid Mech., Tech. Rep. 1999. 24 p.
24. *Raffel M., Willert C.E., Wereley A.T., Kompenhans J.* Particle image velocimetry: a practical guide. Springer-Verlag Berlin Heidelberg, 1998. 253 p.
25. *Adrian R.J.* Particle-imaging techniques for experimental fluid mechanics // Annu. Rev. Fluid Mech. 1991. 23, 261–304. doi: 10.1146/annurev.fluid.23.1.261

References

1. *Prandtl L.* Bemerkungen über den Wärmeübergang im Rohr. *Physik. Zeitschr.* 1928, 29, 487.
2. *Klewicki J.*, *Falco R.* On accurately measuring statistics associated with small-scale structure in turbulent boundary layers using hot-wire probes. *J. Fluid Mech.* 1990, 219, 119–142. doi: 10.1017/S0022112090002889
3. *Balachandar R.*, *Bhuiyan F.* Higher-order moments of velocity fluctuations in an open-channel flow with large bottom roughness. *J. Hydraul. Eng.* 2007, 133(1), 77–87. doi: 10.1061/(ASCE)0733–9429(2007)133:1(77)
4. *Faruque M.A.A.*, *Balachandar R.* Roughness effects on turbulence characteristics in an open channel flow. *Can. J. Civ. Eng.* 2010, 37, 1600–1612. doi: 10.1139/L10–098

5. *Guala M.* et al. Vortex organization in a turbulent boundary layer overlying sparse roughness elements. *J. Hydraul. Res*. 2012, 50(5), 465–481. doi: 10.1080/00221686.2012.729229
6. *Qi M.* et al. Roughness effects on near-wall turbulence modelling for open-channel flows. *J. Hydraul. Res*. 2018, 56(5), 648–661. doi: 10.1080/00221686.2017.1399931
7. *Spiller S.M.* et al. Form-induced stress in non-uniform steady and unsteady open channel flow over a static rough bed. *Int. J. of Sediment Res.* 2015, 30(4), 297–305. doi: 10.1016/j.ijsrc.2014.10.002
8. *Shields A.* Application of similarity principles and turbulence research to bed-load movement. Hydrodynamics Laboratory. Publ. No. 167, *U.S. Dept. of Agr.*, *Soil Conservation Service Cooperative Laboratory*, *California Institute of Technology*, *Pasadena*, *California*.
9. *Hjulstrøm F.* Transportation of debris by moving water. *Recent Marine Sediments*: *A Symposium* / Ed. Trask, P.D. Tulsa, *Oklahoma*, *American Association of Petroleum Geologists*, 1939, 5–31.
10. *van Rijn L.C.* Principles of sediment transport in rivers, estuaries and coastal seas. *Amsterdam*, *Aqua Publications*, 1993. 690 p.
11. *Shvidchenko A.B.*, *Pender G.* Flume study of the effect of relative depth on the incipient motion of coarse uniform sediments. *Water Resour. Research*. 2000, 36, 2, 619–628.
12. *McCarron C.J.*, *Van Landeghem K.J.*, *Baas J.H.*, *Amoudry L.O.*, *Malarkey J.* The hiding-exposure effect revisited: a method to calculate the mobility of bimodal sediment mixtures. *Marine Geology*. 2019, 410, 22–31.
13. *Yang Y.*, *Gao S.*, *Wang Y.P.*, *Jia J.*, *Xiong J.*, *Zhou L.* Revisiting the problem of sediment motion threshold. *Cont. Shelf Res.* 2019, 103960.
14. *Chubarenko I.* et al. Behavior of Microplastics in Coastal Zones. *Microplastic Contamination in Aquatic Environments* / Ed. by Eddy Y. Zeng. *Elsevier*, 2018. P. 175–223. doi: 10.1016/B978–0–12–813747–5.00006–0
15. *Geyer R.*, *Jambeck J.R.*, *Law K.L.* Production, use, and fate of all plastics ever made. *Sci. Adv*. 2017, 3(7), e1700782.
16. *Ballent A.* et al. Modelled transport of benthic marine microplastic pollution in the Nazaré Canyon. *Biogeosciences*. 2013, 10(12), 7957.
17. *Waldschläger K.*, *Schüttrumpf H.* Erosion Behavior of Different Microplastic Particles in Comparison to Natural Sediments. *Env. Sci. Technol.* 2019, 53(22), 13219–13227.
18. *Wilcock P.R.* Methods for estimating the critical shear stress of individual fractions in mixed-size sediment. *Water Resour. Res*. 1988, 24, 1127–1135.
19. *Sherman D.* et al. Sediments and Sediment Transport. *Treatise on Geomorphology* / Ed. by John F. Shroder. *Academic Press*. 2013, 233–256. doi: 10.1016/B978–0–12–374739–6.00013–0
20. *Hinze J.O.* Turbulence: an introduction to its mechanism and theory. *New York*, *McGraw-Hill*, 1959. 586 p.
21. *Wentworth C.K.* A scale of grade and class terms for clastic sediments. *J. Geology*. 1922, 30(5), 377–392.
22. *Sergeev D.A.* A measuring system for studying liquid flows by the particle image velocimetry method based on a diode-pumped solid-state laser. *Instrum. Exp. Tech*. 2009, 52 (3), 438–444. doi: 10.1134/S0020441209030257
23. *Bolinder J.* On the accuracy of digital particle image velocimetry system. *Lund Inst. of Tech.*, *Tech. Div. of Fluid Mech.*, *Tech. Rep*. 1999. 24 p.
24. *Raffel M.*, *Willert C.E.*, *Wereley A.T.*, *Kompenhans J.* Particle image velocimetry: a practical guide. *Springer-Verlag Berlin Heidelberg*, 1998. 253 p.
25. *Adrian R.J.* Particle-imaging techniques for experimental fluid mechanics. *Annu. Rev. Fluid Mech*. 1991, 23, 261–304. doi: 10.1146/annurev.fluid.23.1.261